Electronic Supplementary Material (ESI) for Journal of Materials Chemistry A.

Supporting Information

Design of a Unique Anion Framework in Halospinel for Outstanding Performance of All Solid-state Li-ion Battery: First-principles Approach

Hoje Chun[1], Kyungju Nam[2,3], Sung Jun Hong[1], Joonhee Kang[4*], Byungchan Han[1,2*]

[1] Department of Chemical and Biomolecular Engineering, Yonsei University, Seoul 03722, Republic of Korea

[2] Department of Vehicle Convergence Engineering, Yonsei University, Seoul 03722, Republic of Korea

[3] Institute of Fundamental and Advanced Technology, R&D Division, Hyundai Motor Company, Uiwang 16082, Republic of Korea

[4] Platform Technology Laboratory, Korea Institute of Energy Research, Daejeon 34129, Republic of Korea

- Computational Details
- Tables S1 to S7
- Figures S1 to S5

Table S1. The Haven ratio for $Li_2Sc_{2/3}X_4$ (X = Cl, Br, and I) from AIMD simulation at 800 K.

$Li_2Sc_{2/3}X_4$	Haven ratio
Cl	2.40
Br	0.51
I	0.97

Table S2. Phase equilibria at the interface between $LiCoO_2$ and $Li_2Sc_{2/3}Cl_4$ with the decomposition energies.

Molar fraction	Phase equilibria	Mutual reaction energy (meV/atom)
0	$Li_{17}Sc_5Cl_{32}$	0.00
0.51	ClO_2, Co_3O_4, Sc_2O_3, LiCl	-42.14
0.58	Co_3O_4, $Li(CoO_2)_2$, Sc_2O_3, LiCl	-47.42
1	$LiCoO_2$	0.00

Table S3. Phase equilibria at the interface between $LiCoO_2$ and $Li_2Sc_{2/3}Br_4$ with the decomposition energies.

Molar fraction	Phase equilibria	Mutual reaction energy (meV/atom)
0	$Li_{17}Sc_5Br_{32}$	0.00
0.16	Br, ScBrO, $CoBr_2$, LiBr	-68.02
0.27	Br, ScBrO, CoO, LiBr	-81.53
0.36	Br, CoO, Sc_2O_3, LiBr	-88.72
0.45	Sc_2O_3, Br, Co_3O_4, LiBr	-75.71
1	$LiCoO_2$	0.00

Table S4. Phase equilibria at the interface between $LiCoO_2$ and $Li_2Sc_{2/3}I_4$ with the decomposition energies.

Molar fraction	Phase equilibria	Mutual reaction energy (meV/atom)
0	$Li_{17}Sc_5I_{32}$	0.00
0.16	ScIO, LiI, I, Co	-94.92
0.22	LiI, Sc_2O_3, I, Co	-121.61
0.36	LiI, Sc_2O_3, I, CoO	-142.77
0.43	$LiScO_2$, LiI, I, CoO	-131.25
1	$LiCoO_2$	0.00

Table S5. Phase equilibria at the interface between $LiCoO_2$ and $Li_2Sc_{2/3}Cl_4$ with the decomposition energies under an applied potential of 3 V vs Li metal.

Molar fraction	Phase equilibria	Mutual reaction energy (meV/atom)
0	$ScCl_3$, Cl_2	0.00
0.17	$ScCl_3$, $CoCl_2$, Cl_2O	-112.90
0.30	ClO_2, $ScCl_3$, $CoCl_2$	-115.91
0.79	Co_3O_4, ClO_2, $ScCl_3$	-74.91
0.89	ClO_2, Co_3O_4, Sc_2O_3	-60.55
1	CoO_2	0.00

Table S6. Phase equilibria at the interface between $LiCoO_2$ and $Li_2Sc_{2/3}Br_4$ with the decomposition energies under an applied potential of 3 V vs Li metal.

Molar fraction	Phase equilibria	Mutual reaction energy (meV/atom)
0	$ScBr_3$, Br	0.00
0.16	ScBrO, Br, $CoBr_2$	-121.06

0.27	ScBrO, Br, CoO	-156.91
0.36	Br, CoO, Sc_2O_3	-179.96
0.45	Co_3O_4, Br, Sc_2O_3	-176.51
1	CoO_2	0.00

Table S7. Phase equilibria at the interface between $LiCoO_2$ and $Li_2Sc_{2/3}I_4$ with the decomposition energies under an applied potential of 3 V vs Li metal.

Molar fraction	Phase equilibria	Mutual reaction energy (meV/atom)
0	ScI_3, I	0.00
0.16	ScIO, I, Co	-193.72
0.22	Co, Sc_2O_3, I	-253.91
0.36	Sc_2O_3, CoO, I	-334.50
0.87	Sc_2O_3, CoO, $Co(IO_3)_2$	-212.65
0.90	Co_3O_4, Sc_2O_3, $Co(IO_3)_2$	-201.22
1	CoO_2	0.00

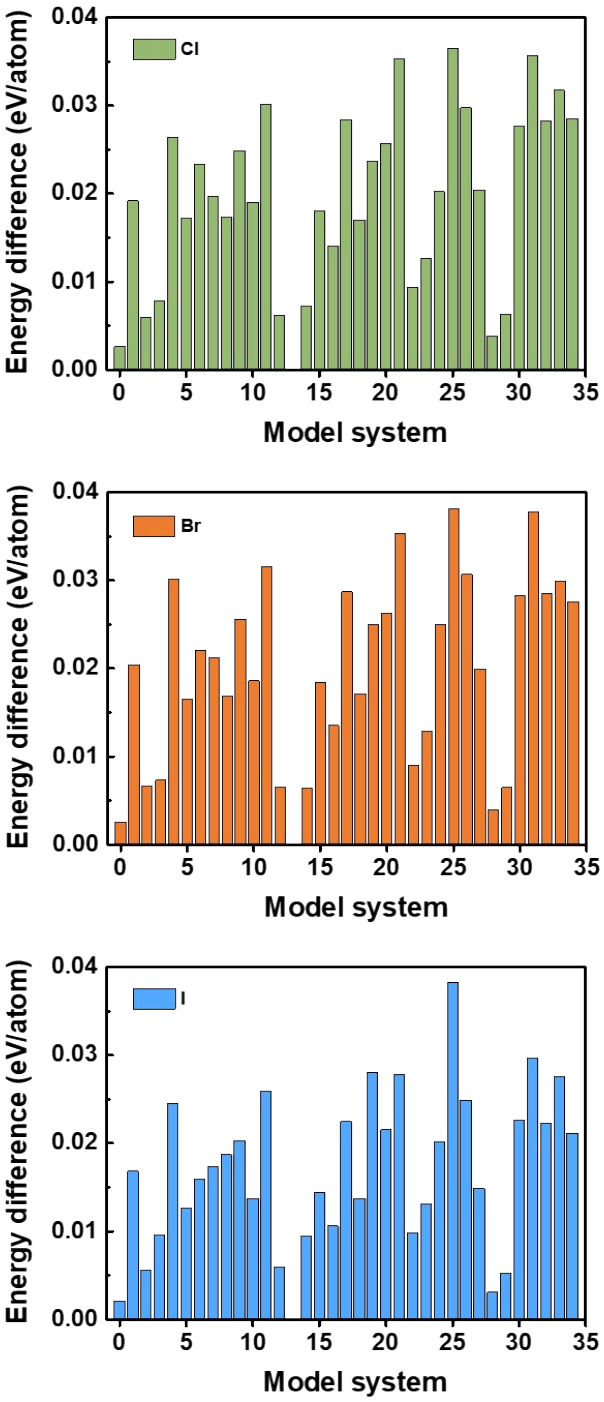

Figure S1. Energy differences of model systems of $Li_{17}Sc_5X_{32}$ (X = Cl, Br, and I) plotted with respect to the structure that is thermodynamically most stable.

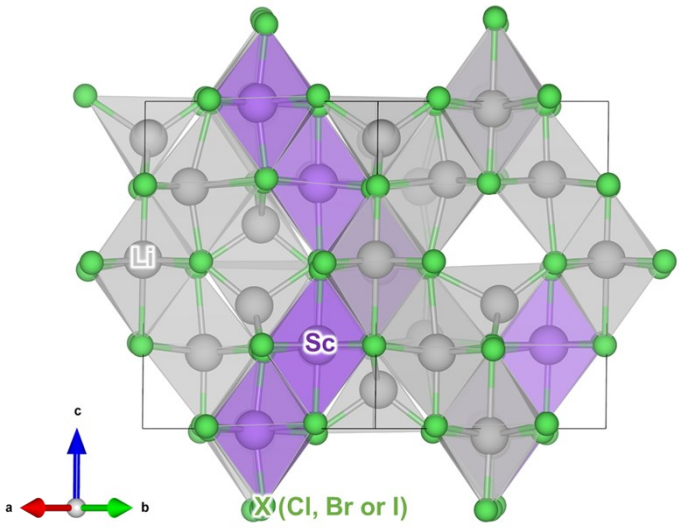

Figure S2. Thermodynamically most unstable structures of $Li_2Sc_{2/3}X_4$.

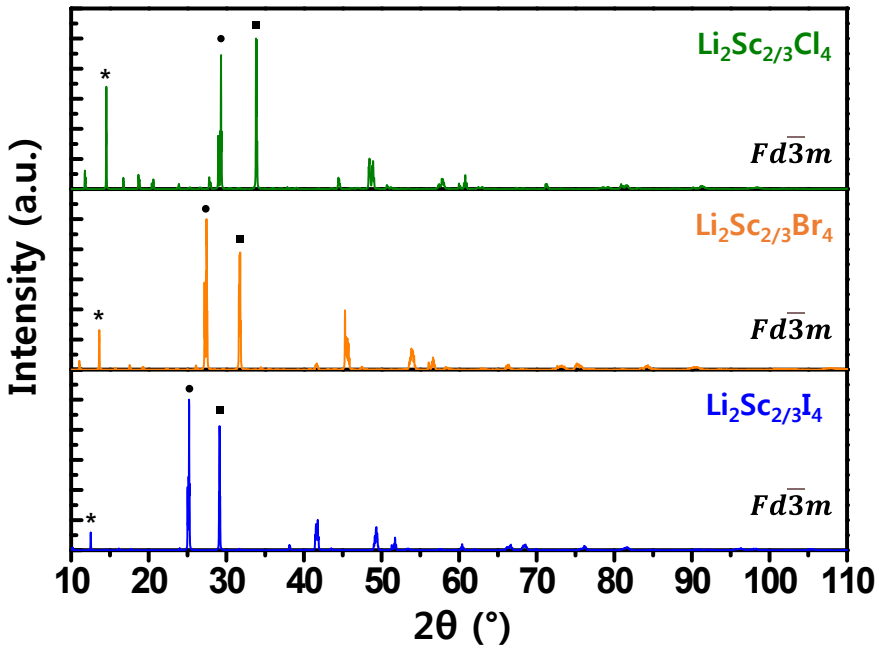

Figure S3. XRD patterns of $Li_2Sc_{2/3}X_4$ (X = Cl, Br, and I). The experimental peaks are marked with symbols.

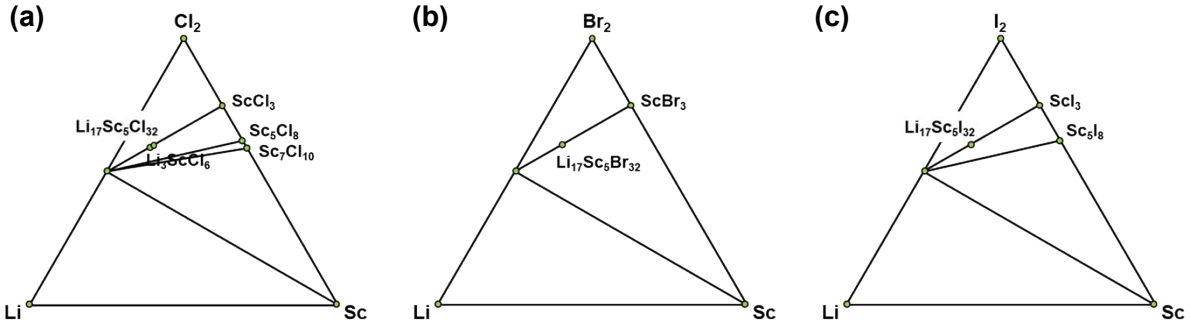

Figure S4. Gibbs triangle of the ternary chemical phase diagram of Li-Sc-X_2 (X = (a) Cl, (b) Br, and (c) I) with formulas of known compounds.

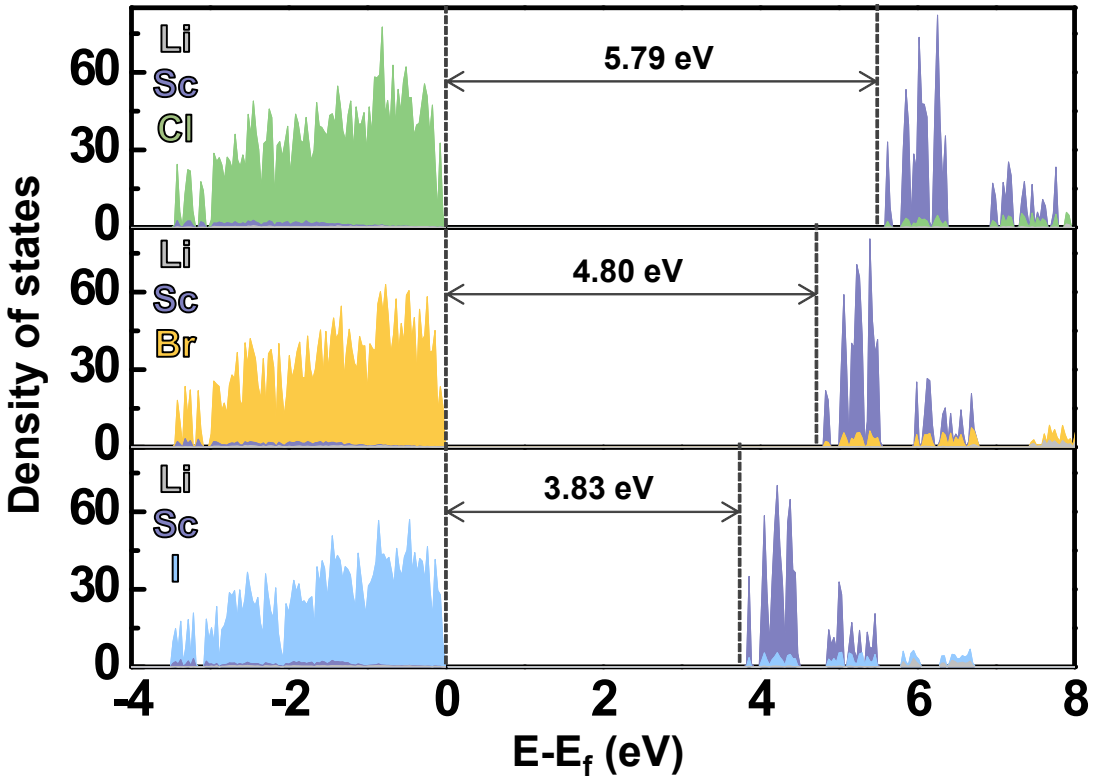

Figure S5. Electronic projected density of states (DOS) of $Li_2Sc_{2/3}X_4$ (X = Cl, Br, and I) using HSE06 hybrid functionals.